Please cite this article in press as: Li et al., Biophysical function of pulmonary surfactant in liquid ventilation, Biophysical Journal (2023), https://doi.org/10.1016/j.bpj.2023.06.014

Biophysical Journal
Article

Biophysical Society

Biophysical function of pulmonary surfactant in liquid ventilation

Guangle Li,[1] Xiaojie Xu,[1] and Yi Y. Zuo[1,2,*]
[1]Department of Mechanical Engineering, University of Hawaii at Manoa, Honolulu, Hawaii and [2]Department of Pediatrics, John A. Burns School of Medicine, University of Hawaii, Honolulu, Hawaii

ABSTRACT Liquid ventilation is a mechanical ventilation technique in which the entire or part of the lung is filled with oxygenated perfluorocarbon (PFC) liquids rather than air in conventional mechanical ventilation. Despite its many ideal biophysicochemical properties for assisting liquid breathing, a general misconception about PFC is to use it as a replacement for pulmonary surfactant. Because of the high PFC-water interfacial tension (59 mN/m), pulmonary surfactant is indispensable in liquid ventilation to increase lung compliance. However, the biophysical function of pulmonary surfactant in liquid ventilation is still unknown. Here, we have studied the adsorption and dynamic surface activity of a natural surfactant preparation, Infasurf, at the PFC-water interface using constrained drop surfactometry. The constrained drop surfactometry is capable of simulating the intra-alveolar microenvironment of liquid ventilation under physiologically relevant conditions. It was found that Infasurf adsorbed to the PFC-water interface reduces the PFC-water interfacial tension from 59 mN/m to an equilibrium value of 9 mN/m within seconds. Atomic force microscopy revealed that after de novo adsorption, Infasurf forms multilayered structures at the PFC-water interface with an average thickness of 10–20 nm, depending on the adsorbing surfactant concentration. It was found that the adsorbed Infasurf film is capable of regulating the interfacial tension of the PFC-water interface within a narrow range, between ~12 and ~1 mN/m, during dynamic compression-expansion cycles that mimic liquid ventilation. These findings have novel implications in understanding the physiological and biophysical functions of the pulmonary surfactant film at the PFC-water interface, and may offer new translational insights into the development of liquid ventilation and liquid breathing techniques.

SIGNIFICANCE Pulmonary surfactant is indispensable to both air-breathing and liquid-breathing lungs for increasing lung compliance. The biophysical function of pulmonary surfactant at the air-water surface is relatively well studied. However, it is largely unknown how pulmonary surfactant film decreases surface tension at the oil-water interface. Here, we report the first biophysical simulation of natural pulmonary surfactant films adsorbed at the perfluorocarbon-water interface using constrained drop surfactometry. It was found that the adsorbed surfactant film regulates the perfluorocarbon-water interfacial tension within a narrow range between 12 and 1 mN/m, during dynamic compression-expansion cycles that mimic liquid ventilation. These findings have novel translational implications into the development of liquid ventilation and liquid breathing techniques.

INTRODUCTION

Liquid ventilation is a mechanical ventilation technique in which the entire lung or part of the lung (usually up to its functional residual capacity) is filled with oxygenated perfluorocarbon (PFC) liquids rather than air in conventional mechanical ventilation (1–4). The feasibility and safety of liquid breathing for mammals were first established in the 1960s (5,6). It has been shown that liquid ventilation with PFCs is able to decrease inflammation, improve pulmonary mechanics, and mitigate injury associated with conventional mechanical ventilation. To date, liquid ventilation has demonstrated improvement in clinical outcome and survival for premature newborns with severe respiratory distress syndrome (7) and for infants with acute respiratory distress syndrome failing to respond to extracorporeal life support (8). Liquid ventilation has also been attempted in adult patients. However, there appears to be insufficient evidence to support its beneficial effect in treating adult patients with acute respiratory distress syndrome (9–12). Although not being used regularly in clinical practice, new paradigm (13) and practice (14) of the liquid ventilation technique have been explored in

Submitted February 19, 2023, and accepted for publication June 20, 2023.
*Correspondence: yzuo@hawaii.edu
Editor: Stephen Hall.
https://doi.org/10.1016/j.bpj.2023.06.014

Please cite this article in press as: Li et al., Biophysical function of pulmonary surfactant in liquid ventilation, Biophysical Journal (2023), https://doi.org/10.1016/j.bpj.2023.06.014

recent years. For instance, Okabe et al. have established the safety and efficacy of PFC-assisted enteral ventilation via the anus in mouse and pig (14). Although the oxygenation mechanism of intestinal breathing remains unclear, PFC-assisted ventilation via the anus appears to be safe and efficacious in improving hypoxia and survival in severe respiratory failure models of mammals, thus providing novel implications to treat COVID-19 patients with respiratory failure (14).

The success of liquid ventilation largely lies in the use of PFCs as an alternative respiratory medium. PFCs, such as perfluorooctane, are hydrocarbons in which all or most of their hydrogen atoms are replaced with fluorine. For perflubron, one bromine atom is added at one end of the hydrocarbon backbone in place of fluorine. PFC liquids are an ideal medium for liquid ventilation because of their superb biophysicochemical properties (15). PFCs have a high oxygen carrying capacity (~50 mL O_2/dL), approximately three times that of hemoglobin, and a high solubility of carbon dioxide (140–210 mL CO_2/dL), thus facilitating gas exchange. In addition, PFCs have a large density (1.7–1.9 g/mL) and a viscosity similar to that of water, which enables delivery of oxygen to the dependent region of the lung and recruitment of atelectasis. Moreover, PFCs are chemically and biologically inert and appear to be safe for internal use. They are mostly cleared from the body with evaporation during exhalation or transpiration through the skin, rather than undergoing metabolism in kidney or liver. After 24 h of liquid ventilation, there is only a low level of PFC residues found in blood and tissues (16).

Among all physicochemical properties of PFC liquids, a crucial property that entails them as the ideal medium for liquid ventilation is their low air-liquid surface tension of 14–18 mN/m (15). This surface tension range is comparable with the equilibrium surface tension of natural pulmonary surfactant (i.e., ~25 mN/m) (17). Hence, it is generally believed that PFCs behave as a replacement for natural pulmonary surfactants during liquid ventilation. However, this point of view has been challenged by two lines of evidence. First, during liquid ventilation, the entire or partial air-water surface of the lung is eliminated and replaced with an oil-water interface between the PFC and the aqueous hypophase of the lung. Hence, the biophysical properties of the PFC-filled lungs should be dominated by the PFC-water interfacial tension, which can be as high as 59 mN/m (18), rather than the low PFC-air surface tension. This hypothesis is supported by ex vivo experimental data. It has been found that the alveolar surface areas of the PFC-filled excised rabbit lungs were significantly smaller than those of the normal air-filled lungs, indicating a high PFC-water interfacial tension that defined the alveolar microstructures of the PFC-filled lungs (19). The maximum interfacial tension of the PFC-filled lungs was estimated at 40 mN/m, significantly higher than the surface tension of PFCs (20,21). Second, pure solvents such as PFCs do not vary their surface or interfacial tension upon surface area variations induced by ventilation or natural inhalation/exhalation cycles. In contrast, an essential biophysical property of the natural pulmonary surfactant is to regulate the dynamic surface tension of alveoli in response to area variations during normal tidal breathing, thus maintaining the alveolar stability (17,22). Therefore, we hypothesized that PFCs do not replace the pulmonary surfactant but play a synergetic role with it to optimize the dynamic surface tension of the lung during liquid ventilation.

Here, for the first time, we report the in vitro dynamic interfacial activity of an animal-derived natural pulmonary surfactant, Infasurf, at the PFC-water interface using a novel experimental methodology called constrained drop surfactometry (CDS), recently developed in our laboratory (18,23). CDS is capable of simulating the intra-alveolar microenvironment of liquid ventilation under physiologically relevant conditions. Using CDS, we found that pulmonary surfactant adsorbed at the PFC-water interface decreases the interfacial tension to an equilibrium value of ~9 mN/m, which is much lower than the equilibrium surface tension of surfactant at the air-water surface, i.e., ~24 mN/m. The adsorbed pulmonary surfactant film regulates the interfacial tension within a narrow range between ~12 and ~1 mN/m during dynamic compression-expansion cycles that mimic liquid ventilation. These findings have novel implications in better understanding the physiological and biophysical functions of the surfactant film at the PFC-water interface, and may offer new translational insights into the development of liquid ventilation and liquid breathing technique.

MATERIALS AND METHODS

Materials

Infasurf (Calfactant) was a gift from ONY Biotech (Amherst, NY). It was prepared from lung lavage of newborn calves with centrifugation and organic extraction. Infasurf contains approximately 90% phospholipid, 5–8% cholesterol, and 2% hydrophobic surfactant proteins, SP-B and SP-C (24). Hydrophilic surfactant proteins, SP-A and SP-D, were removed during the extraction process. Infasurf was stored at −20°C in sterilized vials with a total phospholipid concentration of 35 mg/mL. On the day of experiment, it was diluted to 1 mg/mL using a saline buffer. Perfluorooctane (C_8F_{18}) was purchased from Sigma-Aldrich (St. Louis, MO) and was used without further purification. Water used was Mill-Q ultrapure water (Millipore, Billerica, MA) with a resistivity greater than 18.2 MΩ cm at room temperature.

CDS

CDS is a new generation of droplet-based tensiometry technique developed in our laboratory for studying pulmonary surfactant films at the air-water surface (25,26). We have further developed the CDS technique to allow the study of pulmonary surfactant films at the oil-water interface (18,23). As illustrated in Fig. 1, CDS uses the PFC-water interface of a sessile droplet (oil-in-water configuration) or an inverted pendant drop (water-in-oil configuration) to accommodate the adsorbed surfactant film. The droplet is confined on a carefully machined pedestal with a diameter of 3 mm and knife-sharp edges. To simulate the dynamics of the alveolar lining layer under liquid ventilation, the adsorbed surfactant film can be periodically compressed and expanded at physiologically relevant rates and compression

Please cite this article in press as: Li et al., Biophysical function of pulmonary surfactant in liquid ventilation, Biophysical Journal (2023), https://doi.org/10.1016/j.bpj.2023.06.014

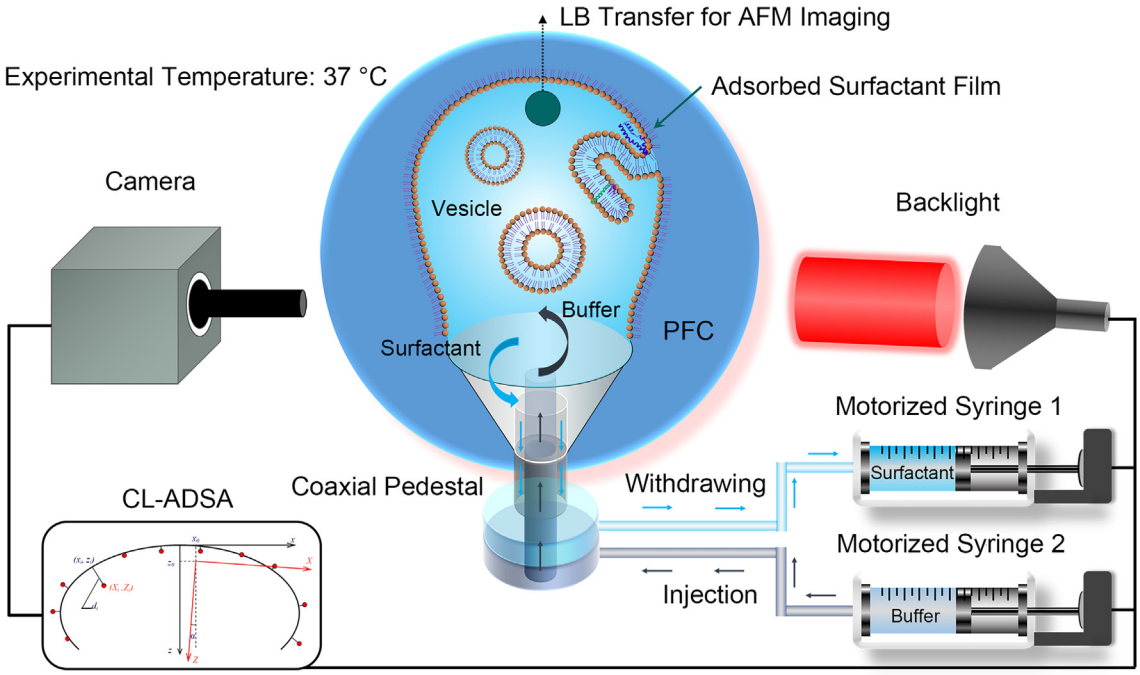

FIGURE 1 Schematic of the CDS. Pulmonary surfactant is adsorbed to the PFC-water interface of a surfactant droplet submerged in PFC. The droplet is constrained on a 3-mm pedestal with knife-sharp edges, and is enclosed in an environmental control chamber maintained at 37°C. Interfacial tension and surface area of the surfactant film are determined simultaneously from the shape of the droplet using closed-loop axisymmetric drop shape analysis (CL-ADSA). Subphase replacement is implemented with a coaxial pedestal connected to two motorized syringes, with one withdrawing the vesicle-containing subphase from the droplet and another one simultaneously injecting buffer into the droplet with the same volumetric rate. The adsorbed surfactant film is subsequently Langmuir-Blodgett (LB) transferred from the PFC-water interface to a freshly peeled mica substrate for atomic force microscopy (AFM) imaging. To see this figure in color, go online.

ratios by precisely controlling liquid flow out of and into the droplet using a motorized syringe. The interfacial tension (γ) and surface area of the pulmonary surfactant film are determined simultaneously from the shape of the droplet using closed-loop axisymmetric drop shape analysis (27). The experimental temperature can be controlled at 37 $\pm$ 0.1°C with a thermoelectric environmental control chamber.

Specifically, the kinetics of Infasurf adsorption to the oil-water interface was studied by recording the adsorption curves (γ versus time) at three phospholipid concentrations, i.e., 0.5, 1, and 1.5 mg/mL, using an oil-in-water (sessile drop) configuration. The PFC droplet ($\sim$7 μL) was formed quickly (within less than a second) in a pool of $\sim$2 mL water using a motorized syringe, to ensure a clean PFC-water interface for surfactant adsorption. The adsorbed surfactant film was subsequently compressed and expanded at three respiratory rates of 12, 6, and 4 cycles/min, respectively, and three compression ratios of 15, 25, and 35%, respectively. At least 10 continuous compression-expansion cycles were recorded for each droplet. Except for the 1st cycle, all remaining cycles generally repeated each other. Biophysical properties of the Infasurf film at the PFC-water interface were quantified, based on results of the 10th cycle, with the minimum interfacial tension (γ_{min}) at the end of compression, and the average isothermal film compressibility, $\kappa = \frac{1}{A}\left(\frac{\partial A}{\partial \gamma}\right)_T$ (17). All results are shown as mean $\pm$ SD ($n = 5$, unless otherwise noted). One-way ANOVA with the Tukey means comparison test was used to determine group differences. $p < 0.05$ was considered to be statistically significant.

Subphase replacement and in situ Langmuir-Blodgett transfer

To directly visualize the lateral structure and molecular conformation of the adsorbed pulmonary surfactant film at the PFC-water interface, we have developed a combined technology of subphase replacement (28) and in situ Langmuir-Blodgett (LB) transfer from the oil-water interface (18). As shown in Fig. 1, subphase replacement from an inverted pendant drop (water-in-oil configuration) was implemented using a coaxial CDS pedestal connected to two motorized syringes, with one withdrawing the phospholipid-vesicle-containing subphase from the droplet at a rate of 0.33 μL/s and the other one simultaneously injecting buffer into the droplet at the same rate. As a result, phospholipid vesicles in the aqueous subphase were washed away without disturbing the adsorbed surfactant film at the oil-water interface, indicated by an unchanged interfacial tension during the subphase replacement process (28). After the subphase replacement, LB transfer of the adsorbed surfactant film was implemented by first quickly inserting a freshly peeled mica sheet into the droplet followed by slowly lifting the mica across the PFC-water interface at a speed of 1 mm/min, under a constant interfacial pressure controlled by the closed-loop axisymmetric drop shape analysis. The deposition ratio of the LB transfer was estimated between 1.1 and 1.4, indicating a complete transfer of the surfactant film from the PFC-water interface to the mica surface (18). Both subphase replacement and LB transfer were performed at 37°C.

Atomic force microscopy

The lateral structure and topography of the adsorbed surfactant film were imaged using an Innova atomic force microscope (AFM) (Bruker, Santa Barbara, CA). Samples were scanned in air using the tapping mode with a silicon cantilever of spring constant 42 mN/m and a resonance frequency of 300 kHz. Samples were scanned at multiple locations to ensure representativeness and reproducibility. Lateral structures were analyzed and three-dimensional renderings were produced using NanoScope Analysis (version 1.5). Height distribution of the surfactant multilayers was estimated with

Please cite this article in press as: Li et al., Biophysical function of pulmonary surfactant in liquid ventilation, Biophysical Journal (2023), https://doi.org/10.1016/j.bpj.2023.06.014

the surface height analysis, i.e., the so-called bearing analysis function of image analysis software. The word "bearing" refers to the differential height between high and low references. The bearing analysis provides the surface height histogram of a feature, by analyzing its surface area and volume above a given reference (29).

RESULTS AND DISCUSSION

Adsorption of Infasurf at the PFC-water interface

Fig. 2 shows the adsorption curves of Infasurf at three different phospholipid concentrations, i.e., 0.5, 1, and 1.5 mg/mL, onto the PFC-water interface at 37°C. Reproducibility of these adsorption curves can be found in Fig. S1 of the supporting material. It can be seen that Infasurf at all three concentrations reaches an equilibrium interfacial tension (γ_{eq}) of ~9 mN/m at the PFC-water interface, corresponding to an equilibrium interfacial pressure ($\pi_{eq} = \gamma_0 - \gamma_{eq}$) of ~50 mN/m, given the interfacial tension of a clean PFC-water interface (γ_0) to be 59 mN/m (18). The γ_{eq} of pulmonary surfactants adsorbed at the air-water surface is ~22–25 mN/m (30), corresponding to a π_{eq} of ~50 mN/m. Hence, although the γ_{eq} of Infasurf adsorbed at the PFC-water interface is much lower than that at the air-water surface, the π_{eq} of Infasurf adsorbed at the PFC-water interface and at the air-water surface is roughly the same. This comparison highlights the physical differences between surface tension and surface pressure. While the γ_{eq} of pulmonary surfactant depends on the actual surface/interface to which the surfactant adsorbs, the π_{eq}, i.e., the relative surface tension between the adsorbing molecules and the surface to which the molecules adsorb, is a physical property of pulmonary surfactants or phospholipids, which is relatively unchanged at ~50 mN/m.

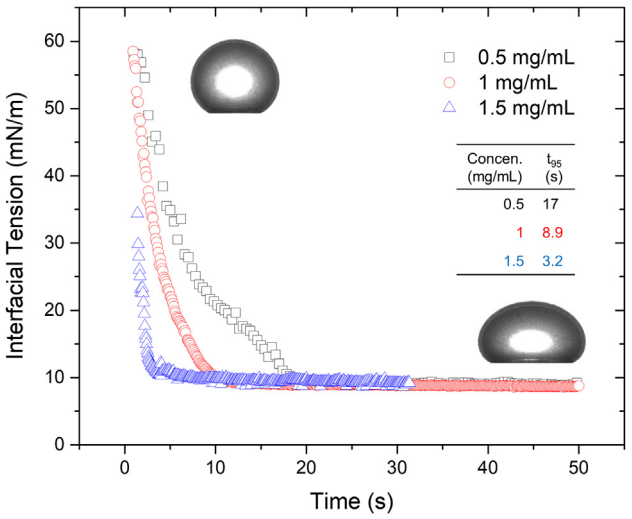

FIGURE 2 Adsorption curves of Infasurf at various concentrations, i.e., 0.5, 1, and 1.5 mg/mL, to the PFC-water interface at 37°C. Insets show typical images of the PFC-in-water (sessile drop) configuration before (59 mN/m) and after Infasurf adsorption (9 mN/m). Also shown in the figure is the adsorption time (t_{95}) for all three surfactant concentrations. To see this figure in color, go online.

Fig. 2 also shows that the adsorption kinetics of Infasurf depends on the phospholipid concentration. Adsorption kinetics can be quantified by the t_{95}, which is the time for the dynamic surface/interfacial tension to drop by 95% from γ_0 to γ_{eq} (31). The t_{95} of Infasurf adsorption to the PFC-water interface is 17, 8.9, and 3.2 s, for 0.5, 1.0, and 1.5 mg/mL, respectively.

Dynamic surface activity of the Infasurf film adsorbed at the PFC-water interface

Fig. 3 shows the dynamic surface activity of the adsorbed Infasurf film (1 mg/mL) at the PFC-water interface at 37°C. Reproducibility of these data can be found in Fig. S2. It has been reported that optimal CO_2 clearance in total liquid ventilation can be achieved with a respiratory rate of 4–5 breaths/min (3,32), which is significantly slower than the respiratory rates used in conventional mechanical ventilation (33). Accordingly, we have simulated three respiratory rates of 4 cycles/min (Fig. 3, *A–C*), 6 cycles/min (Fig. 3, *D–F*), and 12 cycles/min (Fig. 3, *G–I*), with the latter mimicking the respiratory rate of conventional mechanical ventilation.

At the rate of 4 cycles/min, the minimum interfacial tension (γ_{min}) of the Infasurf film gradually reduces to 5, 3, and 1 mN/m, upon 15, 25, and 35% film compression (Fig. 3 *B*). The average compressibility (κ_{comp}) of the Infasurf film increases from 2.0 m/mN at 15% compression, to 3.0 m/mN at 25% compression, and 3.6 m/mN at 35% compression ratio (Fig. 3 *C*). A higher compressibility means that the film requires more area reduction to reduce the surface tension. While a pure dipalmitoyl phosphatidylcholine (DPPC) monolayer in the tilted-condensed phase has a low film compressibility (34), a binary or mixed lipid monolayer consisting of DPPC and other unsaturated phospholipids usually has a relatively high compressibility (24). Hence, these compressibility measurements might indicate that no significant lipid purification or sorting, i.e., the so-called squeeze-out (35), occurs during the dynamic cycling process, similar to surfactant films adsorbed at the air-water surface (28). This is because if squeeze-out gradually occurred during film compression, the film compressibility would have decreased with increasing compression ratio as a consequence of eliminating fluid components from the interfacial monolayer. It should be noted that the characteristic cycles shown in Fig. 3 were not the first but the 10th consecutive compression-expansion cycle. Although the cycles began largely repeating each other after the first cycle (Fig. S2), we cannot rule out the possibility of squeeze-out or lipid purification during the first rapid compression of the film.

Increasing the cycling rate from 4 to 6 cycles/min only slightly decreases the γ_{min} of the Infasurf film from 5 to 4.4 mN/m, upon 15% film compression (Fig. 3 *E*), and

Please cite this article in press as: Li et al., Biophysical function of pulmonary surfactant in liquid ventilation, Biophysical Journal (2023), https://doi.org/10.1016/j.bpj.2023.06.014

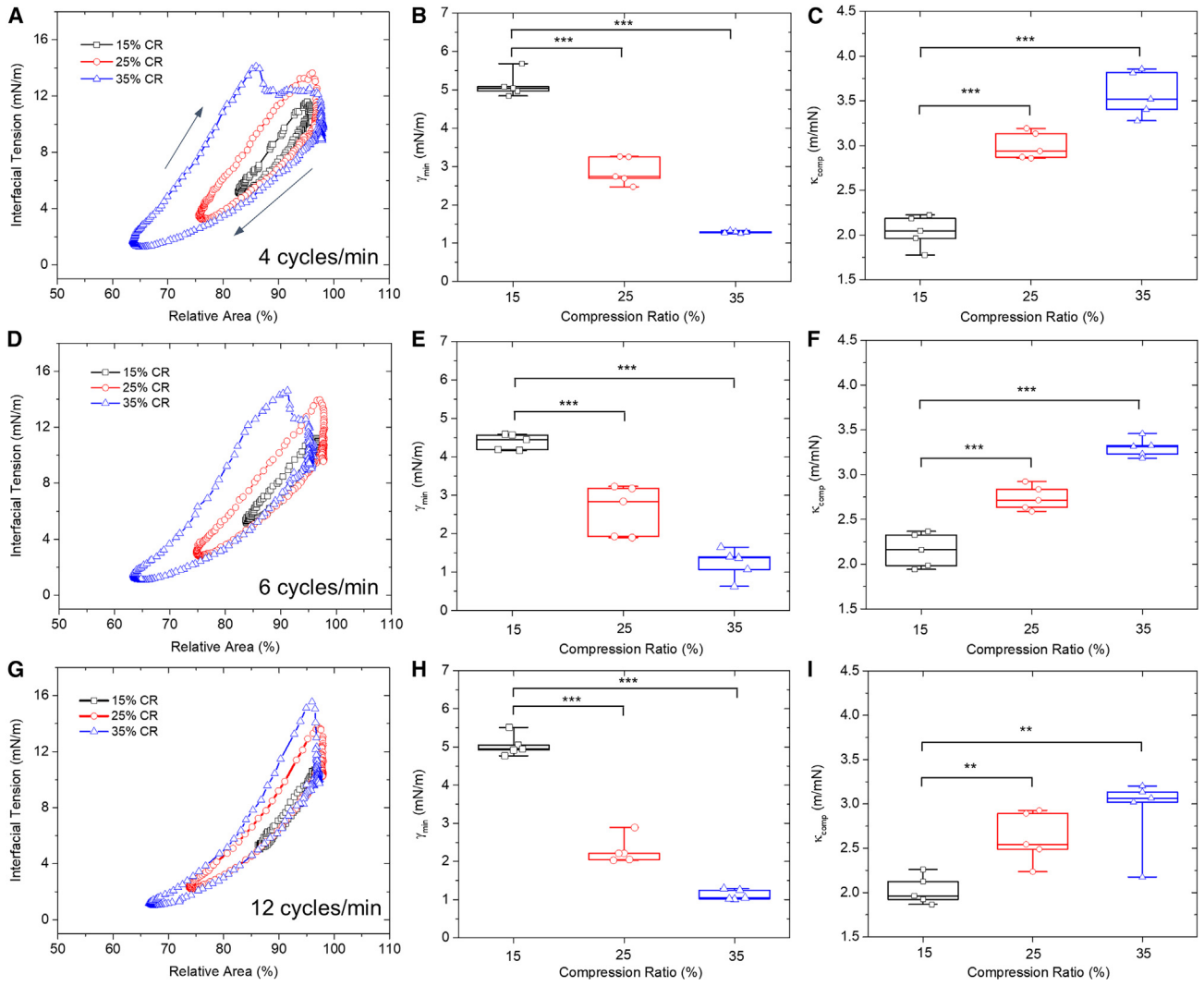

FIGURE 3 Dynamic interfacial tension of 1 mg/mL Infasurf adsorbed to the PFC-water interface at 37°C, with various cycling rates and area compression ratios. Results shown are the typical 10th compression-expansion cycles, minimum interfacial tension (γ_{min}), and film compressibility (κ_{comp}) for mimicking the respiratory rates of 4 breaths/min (*A–C*), 6 breaths/min (*D–F*), and 12 breaths/min (*G–I*). For each cycling rate, three area compression ratios (CRs), i.e., 15, 25, and 35%, were studied. Black arrows in (*A*) indicate the compression and expansion branches of the cycles. $*p < 0.05$, $**p < 0.01$, $***p < 0.001$. To see this figure in color, go online.

slightly reduces the compressibility of the Infasurf film from 3.0 to 2.7 m/mN at 25% compression (Fig. 3 *F*). Further increasing the cycling rate from 6 to 12 cycles/min does not appear to significantly change the γ_{min} and κ_{comp} of the Infasurf film. However, the hysteresis areas of the compression-expansion cycles have been significantly reduced with increasing the cycling rate. Hysteresis area of the compression-expansion cycle indicates energy loss per cycle (17). As shown in Fig. S3, for 35% compression ratio, increasing the cycling rate from 4 to 12 cycles/min reduces the energy loss per cycle by more than 30%, from 0.022 to 0.015 μJ. These results delineate a kinematic effect on the stability of the surfactant film, i.e., increasing the compression rate of the surfactant film increases its stability, as indicated by the reduced hysteresis area. Similar kinematic effects were also found for the surfactant film compressed at the air-water surface (36,37).

Numerous in vitro biophysical simulations using pulsating bubble surfactometry (38), captive bubble surfactometry (39,40), and CDS (25,26) techniques have demonstrated that the dynamic surface tension of natural pulmonary surfactants adsorbed at the air-water surface varies from maximum values of ~30 mN/m (somewhat higher than the γ_{eq} of 25 mN/m) to minimum values close to or less than 1 mN/m (17,22). This range of in vitro surface tension variations for pulmonary surfactant adsorbed at the air-water surface is in good agreement with direct in situ surface tension measurements in excised lungs deflating and inflating between the total lung capacity and the functional residual capacity (41,42).

Please cite this article in press as: Li et al., Biophysical function of pulmonary surfactant in liquid ventilation, Biophysical Journal (2023), https://doi.org/10.1016/j.bpj.2023.06.014

This study shows that Infasurf adsorbed at the PFC-water interface decreases the interfacial tension from ~12 mN/m (somewhat higher than the γ_{eq} = 9 mN/m) to ~1 mN/m during dynamic compression-expansion cycles mimicking the respiratory cycles of liquid ventilation. This range of interfacial tension variations is much smaller than the surface tension variations of the surfactant film adsorbed at the air-water surface undergoing a similar range of film compression, thus indicating a film compressibility fivefold higher than the surfactant film at the air-water surface (~3 vs. 0.6 m/mN) (25,26). This means that it is more difficult for the surfactant film adsorbed at the PFC-water interface to reduce surface tension than that adsorbed at the air-water surface. This is not unexpected since lipid packing at the oil-water interface requires significantly more energy than lipid packing at the air-water surface (43,44).

Lateral structure and topography of the Infasurf film adsorbed at the PFC-water interface

To study the lateral structure and topography of the Infasurf film adsorbed at the PFC-water interface, we first performed subphase replacement in a water-in-oil (inverted pendant drop) configuration to remove the excess lipid vesicles in a 15 μL aqueous droplet of 1 mg/mL Infasurf (Fig. 1). As shown in Figs. S4 and S5, during subphase replacement with one-, two-, three-, and fourfold replacement volumes, the interfacial tension (at the γ_{eq} = 9 mN/m), interfacial area, and volume of the Infasurf droplet remained constant, thus indicating the integrity of the interfacial surfactant film at the PFC-water interface. Fig. 4 shows the lateral structure and topography of the adsorbed Infasurf film after subphase replacement with one-, two-, three-, and fourfold replacement volumes, respectively. Reproducibility of these AFM images with various replacement volumes can be found in Figs. S6–S9. Large unilamellar vesicular structures were found with 1× subphase replacement. These large structures were removed after 2× subphase replacement, indicating that they are nonadsorbing vesicles as a result of inadequate wash with the 1× replacement volume (28). With 3× and 4× subphase replacements, the topographic structures of the Infasurf film appear to be close to those of the Infasurf film with 2× subphase replacement, thus indicating that the 2× replacement volume could be ideal for this subphase replacement process.

In addition to 1 mg/mL Infasurf, we have also studied the lateral structure and topography of the Infasurf film adsorbed to the PFC-water interface, from a high, physiologically relevant phospholipid concentration of 10 mg/mL (45–47). For this high surfactant concentration, it was found that the optimal replacement volume needs to be increased to threefold of the droplet volume (Figs. S10 and S11).

Fig. 5 shows the typical lateral structure and topography of the Infasurf film adsorbed to the PFC-water interface from surfactant concentrations of 1 and 10 mg/mL, respectively. As shown in Fig. 5, *A–D*, the 1 mg/mL Infasurf film shows stacked bilayer structures between 4 and 32 nm in height, corresponding to 1 to 8 bilayer stacks, given the thickness of a fully hydrated phospholipid bilayer to be around 4 nm (48). With bearing analysis of the AFM images, it is found that a majority of multilayer structures have an average height of 10 nm (Fig. 5 *E*). In contrast, the 10 mg/mL Infasurf film shows many more bilayer stacks from 16 to 52 nm in height, corresponding to 4 to 13 stacked bilayers (Fig. 5, *F–I*), with a majority of the multilayers having a height of 20 nm (Fig. 5 *J*).

It is well known that the pulmonary surfactant film adsorbed to the air-water surface is not a monolayer but a

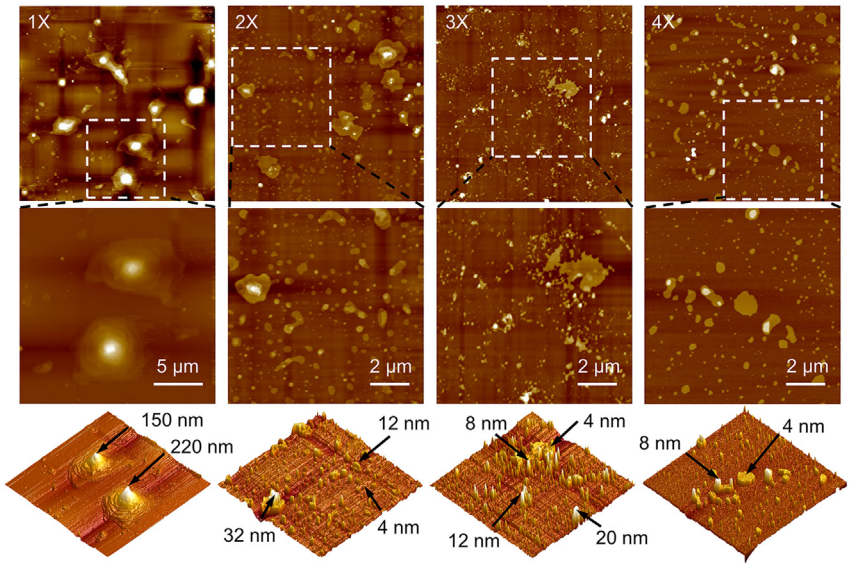

FIGURE 4 Lateral structure and topography of the Infasurf film adsorbed at the PFC-water interface, obtained after subphase replacement with buffer volumes from onefold (1×) to fourfold (4×) of the original droplet volume. The Infasurf concentration is 1 mg/mL. All AFM images in the top row have the same scanning area of 20 × 20 μm, except for 1× (50 × 50 μm). The z range is 400 nm for 1×, 50 nm for 2×, and 20 nm for 3× and 4×. AFM images in the middle row show zoom-in images indicated by the white boxes. AFM images in the bottom row show the 3D rendering of the zoom-in images. Single-headed black arrows indicate the heights of structures. To see this figure in color, go online.

Please cite this article in press as: Li et al., Biophysical function of pulmonary surfactant in liquid ventilation, Biophysical Journal (2023), https://doi.org/10.1016/j.bpj.2023.06.014

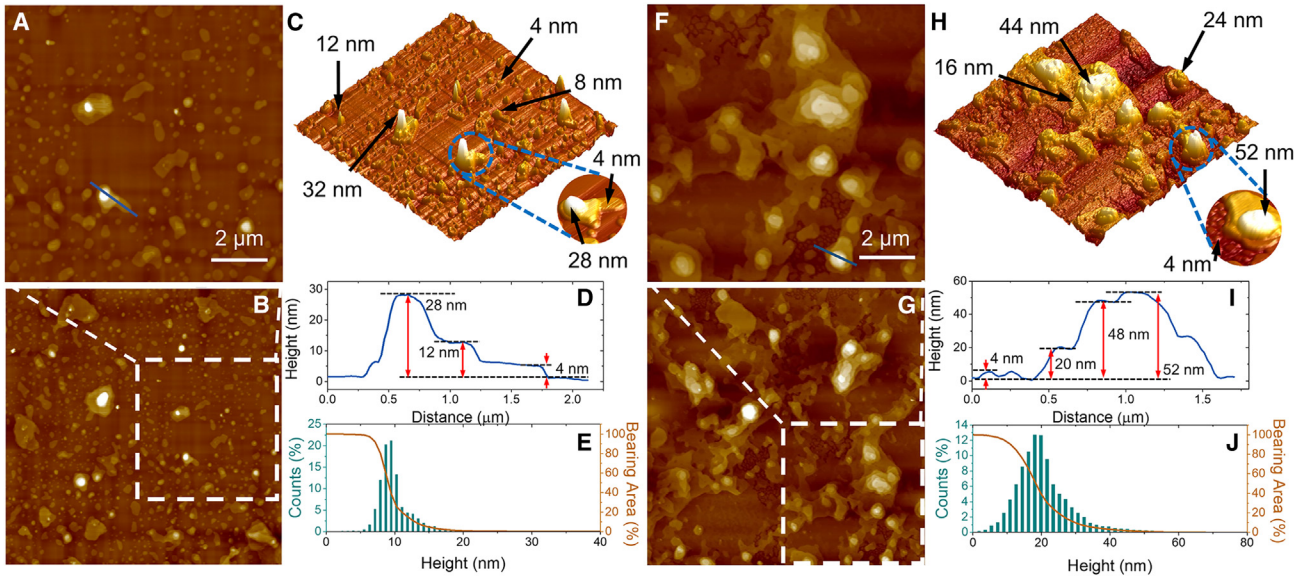

FIGURE 5 Lateral structure and topography of the Infasurf film adsorbed at the PFC-water interface from surfactant concentrations of 1 mg/mL (*A–E*) and 10 mg/mL (*F–J*). AFM images shown in (*A* and *F*) have the same scanning area of 10 × 10 μm. The *z* range is 50 nm for 1 mg/mL Infasurf and 100 nm for 10 mg/mL Infasurf. (*B* and *G*) Zoom-out images indicated by the white boxes. (*C* and *H*) 3D renderings of (*A* and *F*). Detailed multilayer structures are shown in circles. Single-headed black arrows indicate the heights of structures. (*D* and *I*) Height profiles of a cross section corresponding to the blue lines drawn in (*A* and *F*). (*E* and *J*) Height histogram and bearing area curve of the multilayered structures shown in (*B* and *G*). The bearing area curve is the integral of the surface height histogram, which shows the area percentage of the surface above a reference plane as a function of the depth of that plane below the highest point in the image. To see this figure in color, go online.

multilayer with an interfacial monolayer at the air-water surface, plus multilayered structures closely and functionally attached to the interfacial monolayer (39,40). Theoretical models of pulmonary surfactant suggested that multilayer formation by collapse of the interfacial monolayer might be a necessity to mimic the ultralow surface tension of pulmonary surfactant at the air-water surface (49). Our previous study has further demonstrated that the interfacial monolayer of adsorbed pulmonary surfactant film is highly enriched in DPPC, and hence there should be no or only very limited lipid purification or sorting at the interfacial monolayer after de novo adsorption (28). The multilayered structures formed by de novo adsorption of 1 mg/mL Infasurf to the air-water surface were found to have an average thickness of 28 nm (28), which is nearly three times the average height of the 1 mg/mL Infasurf adsorbed to the PFC-water interface. These topographic differences indicate that the pulmonary surfactant film experiences a much larger energy barrier for folding or forming multilayer protrusions at the oil-water interface than at the air-water surface, likely due to the much stronger steric and/or hydrophobic restrictions for lipid motion at the oil-water interface (43,44).

Previously, we reported the lateral structure and topography of the spread Infasurf monolayer under a quasistatic compression at room temperature (23). The purpose of that study was to understand the physical chemistry and phase transitions of the spread surfactant film under nonphysiologically relevant conditions. It was found that the pulmonary surfactant film spread at the PFC-water interface undergoes phase transitions at surface pressures less than the equilibrium spreading pressure of 50 mN/m (23), corresponding to the equilibrium surface tension of 9 mN/m found here. Specifically, the Infasurf monolayer spread at the PFC-water interface undergoes a monolayer-to-multilayer transition at a surface pressure of 50 mN/m, to form multilayered protrusions 4–8 nm in height (23), which are generally smaller than the multilayers found in the adsorbed Infasurf film (Fig. 5).

In contrast, the purpose of this study is to gain insight into the biophysical properties and lateral structures of the surfactant film under physiologically relevant conditions, such as dynamic cycling of the surfactant film at 37°C, and the surfactant film adsorbed from physiologically relevant high surfactant concentrations (Fig. 5). Such a study was made feasible owing to our recent technological advance in the development of a subphase replacement technique in CDS (28). The morphological comparison between the spread and adsorbed Infasurf films at the PFC-water interface suggests that administration of high-concentration exogenous surfactant bolus may significantly benefit lung recruitment of patients on liquid ventilation. Exogenous surfactant is of particular importance under conditions that liquid ventilation becomes a necessity, at which the endogenous surfactant of the patients is deemed to be deficient or seriously inactivated. After administration of the exogenous

surfactant and its adsorption, the multilayered pulmonary surfactant film is responsible for regulating the interfacial tension of the PFC-water interface within a range between 1 and 12 mN/m, corresponding to respiratory cycles of the liquid ventilation. This finding is consistent with a number of in vivo studies that showed exogenous surfactants given before liquid ventilation improved the pathological outcomes (20,21,50,51).

CONCLUSIONS

We have studied the adsorption and dynamic surface activity of a modified natural pulmonary surfactant, Infasurf, at the PFC-water interface using CDS. The CDS is capable of simulating the intra-alveolar microenvironment of liquid ventilation under physiologically relevant conditions. Our data suggest that PFC alone does not behave as a surfactant replacement in liquid ventilation. Infasurf at 1 mg/mL adsorbed to the PFC-water interface reduces the PFC-water interfacial tension from 59 mN/m to an equilibrium value of 9 mN/m within seconds. Atomic force microscopy revealed that, after de novo adsorption, Infasurf forms multilayered structures at the PFC-water interface with an average thickness of 10–20 nm, depending on the adsorbing surfactant concentration. Most importantly, the adsorbed Infasurf film is capable of regulating the interfacial tension of the PFC-water interface within a narrow range, between $\sim$12 and $\sim$1 mN/m, during dynamic compression-expansion cycles that mimic liquid ventilation. These findings have novel implications in better understanding the physiological and biophysical functions of the pulmonary surfactant film at the PFC-water interface, and may offer new translational insights into the development of liquid ventilation and liquid breathing techniques.

SUPPORTING MATERIAL

Supporting material can be found online at https://doi.org/10.1016/j.bpj.2023.06.014.

AUTHOR CONTRIBUTIONS

G.L and X.X. carried out the experiments and data analysis. Y.Y.Z. designed the research and oversaw the experiments and analysis. Y.Y.Z. and G.L. wrote the paper. All authors discussed the results.

ACKNOWLEDGMENTS

We thank Dr. Sindhu Row of ONY Biotech for donation of Infasurf samples. This research was supported by the National Science Foundation grant no. CBET-2011317 (to Y.Y.Z.).

DECLARATION OF INTERESTS

The authors declare no competing interests.

REFERENCES

1. Kaisers, U., K. P. Kelly, and T. Busch. 2003. Liquid ventilation. *Br. J. Anaesth.* 91:143–151.
2. Wolfson, M. R., and T. H. Shaffer. 2005. Pulmonary applications of perfluorochemical liquids: ventilation and beyond. *Paediatr. Respir. Rev.* 6:117–127.
3. Tawfic, Q. A., and R. Kausalya. 2011. Liquid ventilation. *Oman Med. J.* 26:4–9.
4. Eichenwald, C., K. Dysart, …, W. Fox. 2020. Neonatal Partial Liquid Ventilation for the Treatment and Prevention of Bronchopulmonary Dysplasia. *NeoReviews.* 21:e238–e248.
5. Kylstra, J. A., M. O. Tissing, and A. van der Maen. 1962. Of mice as fish. *Trans. Am. Soc. Artif. Intern. Organs.* 8:378–383.
6. Clark, L. C., Jr., and F. Gollan. 1966. Survival of mammals breathing organic liquids equilibrated with oxygen at atmospheric pressure. *Science.* 152:1755–1756.
7. Leach, C. L., J. S. Greenspan, …, B. P. Fuhrman. 1996. Partial liquid ventilation with perflubron in premature infants with severe respiratory distress syndrome. The LiquiVent Study Group. *N. Engl. J. Med.* 335:761–767.
8. Greenspan, J. S., W. W. Fox, …, T. H. Shaffer. 1997. Partial liquid ventilation in critically ill infants receiving extracorporeal life support. Philadelphia Liquid Ventilation Consortium. *Pediatrics.* 99:E2.
9. Hirschl, R. B., T. Pranikoff, …, R. H. Bartlett. 1996. Initial experience with partial liquid ventilation in adult patients with the acute respiratory distress syndrome. *JAMA.* 275:383–389.
10. Hirschl, R. B., M. Croce, …, R. H. Bartlett. 2002. Prospective, randomized, controlled pilot study of partial liquid ventilation in adult acute respiratory distress syndrome. *Am. J. Respir. Crit. Care Med.* 165:781–787.
11. Kacmarek, R. M., H. P. Wiedemann, …, A. S. Slutsky. 2006. Partial liquid ventilation in adult patients with acute respiratory distress syndrome. *Am. J. Respir. Crit. Care Med.* 173:882–889.
12. Galvin, I. M., A. Steel, …, M. W. Davies. 2013. Partial liquid ventilation for preventing death and morbidity in adults with acute lung injury and acute respiratory distress syndrome. *Cochrane Database Syst. Rev.* 2013:CD003707.
13. Kohlhauer, M., E. Boissady, …, R. Tissier. 2020. A new paradigm for lung-conservative total liquid ventilation. *EBioMedicine.* 52, 102365.
14. Okabe, R., T. F. Chen-Yoshikawa, …, T. Takebe. 2021. Mammalian enteral ventilation ameliorates respiratory failure. *Med.* 2:773–783.e5.
15. Wolfson, M. R., and T. H. Shaffer. 2004. Liquid ventilation: an adjunct for respiratory management. *Paediatr. Anaesth.* 14:15–23.
16. Shaffer, T. H., M. R. Wolfson, and J. S. Greenspan. 1999. Liquid ventilation: current status. *Pediatr. Rev.* 20:e134–e142.
17. Zuo, Y. Y., R. A. W. Veldhuizen, …, F. Possmayer. 2008. Current perspectives in pulmonary surfactant — Inhibition, enhancement and evaluation. *Biochim. Biophys. Acta.* 1778:1947–1977.
18. Li, G., X. Xu, and Y. Y. Zuo. 2023. Langmuir-Blodgett transfer from the oil-water interface. *J. Colloid Interface Sci.* 630:21–27.
19. Bachofen, H., S. Schürch, and F. Possmayer. 1994. Disturbance of alveolar lining layer: effects on alveolar microstructure. *J. Appl. Physiol.* 76:1983–1992.
20. Tarczy-Hornoch, P., J. Hildebrandt, …, J. C. Jackson. 1996. Effects of exogenous surfactant on lung pressure-volume characteristics during liquid ventilation. *J. Appl. Physiol.* 80:1764–1771.
21. Tarczy-Hornoch, P., J. Hildebrandt, …, J. C. Jackson. 1998. Surfactant replacement increases compliance in premature lamb lungs during partial liquid ventilation in situ. *J. Appl. Physiol.* 84:1316–1322.
22. Autilio, C., and J. Pérez-Gil. 2019. Understanding the principle biophysics concepts of pulmonary surfactant in health and disease. *Arch. Dis. Child. Fetal Neonatal Ed.* 104:F443–F451.

23. Li, G., X. Xu, and Y. Y. Zuo. 2023. Phase transitions of the pulmonary surfactant film at the perfluorocarbon-water interface. *Biophys. J.* 122:1772–1780.
24. Zhang, H., Q. Fan, …, Y. Y. Zuo. 2011. Comparative study of clinical pulmonary surfactants using atomic force microscopy. *Biochim. Biophys. Acta.* 1808:1832–1842.
25. Valle, R. P., T. Wu, and Y. Y. Zuo. 2015. Biophysical Influence of Airborne Carbon Nanomaterials on Natural Pulmonary Surfactant. *ACS Nano.* 9:5413–5421.
26. Yang, Y., Y. Wu, …, Y. Y. Zuo. 2018. Biophysical Assessment of Pulmonary Surfactant Predicts the Lung Toxicity of Nanomaterials. *Small Methods.* 2, 1700367.
27. Yu, K., J. Yang, and Y. Y. Zuo. 2016. Automated Droplet Manipulation Using Closed-Loop Axisymmetric Drop Shape Analysis. *Langmuir.* 32:4820–4826.
28. Xu, L., Y. Yang, and Y. Y. Zuo. 2020. Atomic Force Microscopy Imaging of Adsorbed Pulmonary Surfactant Films. *Biophys. J.* 119:756–766.
29. Higo, M., T. Futagawa, …, Y. Ozono. 2003. Adsorption State and Morphology of Tetracyanoquinodimethane Deposited from Solution onto the Atomically Smooth Native Oxide Surface of Al(111) Films Studied by X-i.e. Photoelectron Spectroscopy and Atomic Force Microscopy. *J. Phys. Chem. B.* 107:5871–5876.
30. Bai, X., L. Xu, …, G. Hu. 2019. Adsorption of Phospholipids at the Air-Water Surface. *Biophys. J.* 117:1224–1233.
31. Zuo, Y. Y., R. Gitiafroz, …, A. W. Neumann. 2005. Effect of humidity on the adsorption kinetics of lung surfactant at air-water interfaces. *Langmuir.* 21:10593–10601.
32. Pohlmann, J. R., D. O. Brant, …, R. B. Hirschl. 2011. Total liquid ventilation provides superior respiratory support to conventional mechanical ventilation in a large animal model of severe respiratory failure. *ASAIO J.* 57:1–8.
33. Lellouche, F., M. Delorme, and L. Brochard. 2020. Impact of Respiratory Rate and Dead Space in the Current Era of Lung Protective Mechanical Ventilation. *Chest.* 158:45–47.
34. Kaganer, V. M., H. Möhwald, and P. Dutta. 1999. Structure and phase transitions in Langmuir monolayers. *Rev. Mod. Phys.* 71:779–819.
35. Keating, E., Y. Y. Zuo, …, R. A. W. Veldhuizen. 2012. A modified squeeze-out mechanism for generating high surface pressures with pulmonary surfactant. *Biochim. Biophys. Acta.* 1818:1225–1234.
36. Smith, E. C., J. M. Crane, …, S. B. Hall. 2003. Metastability of a supercompressed fluid monolayer. *Biophys. J.* 85:3048–3057.
37. Crane, J. M., and S. B. Hall. 2000. Stability of pulmonary surfactant monolayers depends on rate of compression. *Am J Resp Crit Care Med.* 161:A660.
38. Enhorning, G. 2001. Pulmonary surfactant function studied with the pulsating bubble surfactometer (PBS) and the capillary surfactometer (CS). *Comp. Biochem. Physiol. Mol. Integr. Physiol.* 129:221–226.
39. Schürch, S., F. H. Green, and H. Bachofen. 1998. Formation and structure of surface films: captive bubble surfactometry. *Biochim. Biophys. Acta.* 1408:180–202.
40. Schürch, S., H. Bachofen, and F. Possmayer. 2001. Surface activity in situ, in vivo, and in the captive bubble surfactometer. *Comp. Biochem. Physiol. Mol. Integr. Physiol.* 129:195–207.
41. Schürch, S., J. Goerke, and J. A. Clements. 1978. Direct determination of volume- and time-dependence of alveolar surface tension in excised lungs. *Proc. Natl. Acad. Sci. USA.* 75:3417–3421.
42. Schürch, S. 1982. Surface tension at low lung volumes: dependence on time and alveolar size. *Respir. Physiol.* 48:339–355.
43. Pichot, R., R. L. Watson, and I. T. Norton. 2013. Phospholipids at the interface: current trends and challenges. *Int. J. Mol. Sci.* 14:11767–11794.
44. Li, G., and Y. Y. Zuo. 2022. Molecular and colloidal self-assembly at the oil–water interface. *Curr. Opin. Colloid Interface Sci.* 62, 101639.
45. Lewis, J. F., and A. H. Jobe. 1993. Surfactant and the adult respiratory distress syndrome. *Am. Rev. Respir. Dis.* 147:218–233.
46. Ikegami, M., C. M. Rebello, and A. H. Jobe. 1996. Surfactant inhibition by plasma: gestational age and surfactant treatment effects in preterm lambs. *J. Appl. Physiol.* 81:2517–2522.
47. Rebello, C. M., A. H. Jobe, …, M. Ikegami. 1996. Alveolar and tissue surfactant pool sizes in humans. *Am. J. Respir. Crit. Care Med.* 154:625–628.
48. Marsh, D. 1990. CRC handbook of lipid bilayers.
49. Krueger, M. A., and D. P. Gaver, 3rd.. 2000. A Theoretical Model of Pulmonary Surfactant Multilayer Collapse under Oscillating Area Conditions. *J. Colloid Interface Sci.* 229:353–364.
50. Mrozek, J. D., K. M. Smith, …, M. C. Mammel. 1997. Exogenous surfactant and partial liquid ventilation: physiologic and pathologic effects. *Am. J. Respir. Crit. Care Med.* 156:1058–1065.
51. Nishina, K., K. Mikawa, …, H. Obara. 2005. The efficacy of fluorocarbon, surfactant, and their combination for improving acute lung injury induced by intratracheal acidified infant formula. *Anesth. Analg.* 100:964–971.